Equivalent Model of a Synchronous PV Power Plant

Daniel Remon*‡, Antoni M. Cantarellas*‡, Mohamed Atef Abbas Elsaharty‡,
Cosmin Koch-Ciobotaru*, Pedro Rodriguez*‡
*Abengoa Research, Abengoa
Campus Palmas Altas, Seville, Spain 41014
Email: daniel.remon@abengoa.com
‡Department of Electrical Engineering
Technical University of Catalonia
GAIA Building, Terrassa, Barcelona, Spain 08222

***Abstract*—The continuous integration of renewable energy sources into power systems has led to the construction of large power plants based on power electronics, with power ratings up to hundreds of megawatts, in order to accomodate technologies like solar PV and wind energy. Due to the size of these plants, they must provide support services for the grid and it is necessary to analyze the impact they have on power systems.**

Opposing to conventional power plants formed by a reduced number of synchronous generators in the range of several hundreds of megawatts, large power plants based on PV and wind energy are usually composed of a high number of individual generating units with power ratings of a few megawatts. Therefore, it is of great importance to develop aggregated models of power plants formed by multiple power converters to be used in the dynamic analysis of large power systems. This paper presents the control system of a 20 MW PV plant, derives an equivalent aggregated model and studies the performance of this model through simulation.

***Index Terms*—grid support, power plant equivalent, power system stability, renewable energy sources.**

I. Introduction

The participation of renewable energy sources in power systems is reportedly increasing and this trend is expected to be maintained during the next years due to environmental concern and technology cost reduction [1]. In fact, these sources are not only used in small residential installations, but they also contribute to large scale power generation through plants that may reach power ratings over 100 MW. This is the case of many concentrated solar power plants employing synchronous generators, but also of some solar PV or wind power plants based on power electronics converters.

Generating units connected to electrical grids through power electronics do not usually behave dynamically like synchronous generators, which give classical power systems their main characteristics [2]. Basically, synchronous machines can be seen as a voltage source behind an impedance, and are able to energize an electrical system in order to form a grid, and to maintain its voltage. Furthermore, they work in synchronism with the grid in a natural way, and their inertia counteracts any frequency variations that may occur because of supply and demand imbalances.

This work has been partially supported by the Spanish Ministry of Science and Innovation under the project ENE2014-60228-R.

Any opinions, findings and conclusions or recommendations expressed in this material are those of the authors and do not necessarily reflect those of the host institutions or funders.

However, power electronics converters do not have these properties by themselves. Therefore, and specially when power plants in the range of 100 MW are considered, it is necessary to analyze the impact that plants using power electronics may have on power systems. For that purpose, it is essential to study new control concepts that allow them to interact harmoniously with power systems, and to contribute to their control as required by system operators [3].

Among the main concerns of power system operators it is possible to cite the contribution of these new plants to frequency and voltage regulation, the provision of inertia for the power system or the damping of power oscillations. This is particularly necessary when this type of power plants replaces conventional generating units employing synchronous generators that provide grid support services. As a solution, many authors have proposed emulating to some extent the behavior of synchronous machines in the control systems of power converters [4]–[7]. Among them, the synchronous power controller (SPC) presented in [7] is a very flexible solution that considers the swing equation of a synchronous machine and improves the damping of its response.

On the other hand, the analysis of power systems usually involves a large number of generating units with power ratings in the range of several hundreds of megawatts, whereas large power plants based on power electronics are normally formed by a large quantity of small units, whose power rating is around 1 MW. Although the use of a detailed model may provide very useful information in a dynamic analysis, it can also lead to unnecessarily long simulation times and, in the worst case, to numerical issues due to the use of different scales. Therefore, it is interesting to develop equivalent models of distributed power plants that aggregate different generating units, reducing the number of units considered in the analysis and increasing their power.

This paper presents an aggregated model of a PV power plant formed by 20 power converters rated at 1 MW using the SPC. The remaining sections are organized as follows. Section

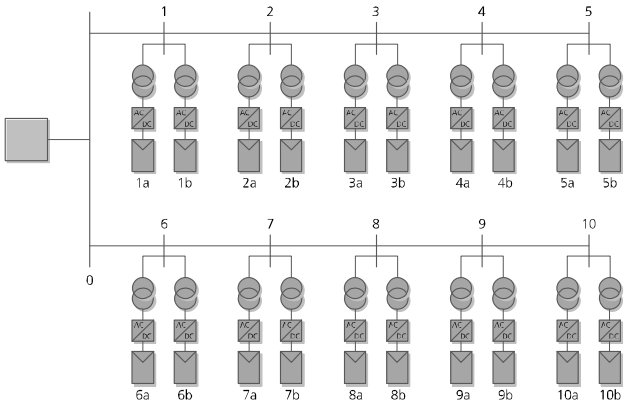

Fig. 1. Single-line diagram of the power plant.

TABLE I
CHARACTERISTICS OF CABLES

Cable	L (m)	R (Ω)	X (Ω)	C (uF)	I_r (kA)
0-1, 0-6	600	0.04590	0.07518	0.1158	0.440
1-2, 6-7	250	0.01913	0.03133	0.04825	0.440
2-3, 7-8	250	0.03118	0.03385	0.04150	0.350
3-4, 8-9	250	0.03118	0.03385	0.04150	0.350
4-5, 9-10	250	0.04823	0.03620	0.03650	0.281

II presents the power plant and its control system, explaining the fundamentals of the synchronous power controller. In section III, an equivalent model is derived through the aggregation of the whole plant in a single 20 MW converter. Afterwards, the equivalent model is compared with the detailed model of the plant through simulation in DIgSILENT PowerFactory in section IV. Finally, the main conclusions are summarized in section V.

II. Power Plant Structure and Control

A. Power Plant Structure

The PV power plant studied in this paper is connected to a 50 Hz, 33 kV grid and is formed by 20 PV generating stations equally distributed over two identical feeders, as shown in Fig. 1. Each feeder connects five buses to the point of common coupling of the plant and, at each bus, two generating stations are connected through independent $33/0.365$ kV transformers.

The section and length of the cables varies according to the plant layout and their power transfer requirements and their main characteristics are summarized in Table I. The transformers, with a rated power of 1.15 MVA, have a short circuit voltage $\varepsilon_{cc} = 9\%$ and copper losses of 3.45 kW.

The generating stations are formed by one power converter whose rated voltage and power are respectively 365 V and 1.25 MVA, designed to operate at a 0.8 power factor, and the corresponding PV array with a peak power of 1.2 MW. The converters are connected to the grid through an LCL filter that mitigates the harmonic injection.

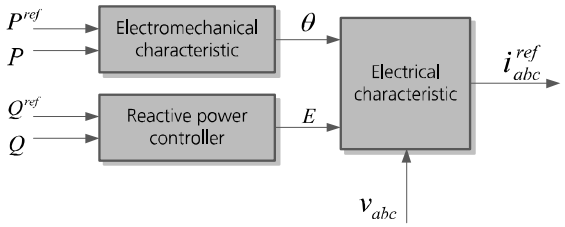

Fig. 2. Constituting blocks of the synchronous power controller.

B. Power Plant Control

The static control of the power plant, i.e., how references are shared among the different stations, can be performed in different ways. For instance, it is possible to divide active and reactive power references in equal parts, so that all stations contribute in the same proportion, or an optimization algorithm can be run to exploit the plant optimally taking into account the state of different elements and the availability of the resource at different points of the plant. Since this paper focuses on the dynamic behavior of the plant, a simple strategy based on constant participation factors is defined to share the active and reactive power references. These participation factors are not necessarily equal for all the stations. Apart from this, the plant contributes to frequency and voltage regulation with a droop response such that each station measures frequency and voltage at its 365 V bus and responds independently.

The dynamic response of the plant is also the result of the independent response of all the stations. Due to the speed of power converters, the response of each station depends on its control loops, as explained in the following.

1) Inner controllers: The converters work with a pulse width modulation that generates the pulses for the power switches. The modulation follows a converter voltage reference provided by a current controller that ensures the current injected after the filter tracks the reference provided by the outer controller. The fast response of the converter and the current loop makes possible to model the converter and its inner control loops as a controlled current source that injects the current reference with a short delay represented by a first-order low-pass filter with a time constant $\tau = 5$ ms.

2) The synchronous power controller: The outer controller generating the current reference is in this case the synchronous power controller [7]. The SPC reproduces a simplified electrical model and the swing equation of a virtual synchronous machine and is mainly constituted by three blocks, as depicted in Fig. 2.

The electrical characteristic of the SPC contains a simplified model of an electrical machine, where it is seen as a voltage source behind an impedance, as shown in Fig. 3. Using the values of the internal voltage magnitude and angle respectively provided by the reactive power controller and the electromechanical characteristic blocks, it generates the current to be injected by the converter.

In order to do that, the voltage drop through the virtual

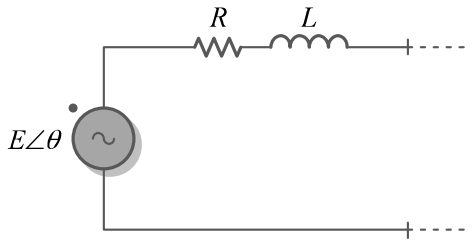

Fig. 3. Simplified electrical equivalent of a synchronous machine.

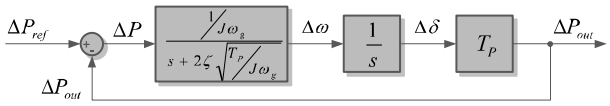

Fig. 4. Active power loop with the synchronous power controller emulating inertia J with damping coefficient ζ.

impedance in Fig. 3 is calculated, which requires taking the difference between the internal voltage and the grid voltage. In each phase, this voltage drop induces a current that is given by (1). In small signal, the current is obtained from the corresponding voltage drop as in (2).

$$\frac{di}{dt} = \frac{1}{L}\left(\Delta v - Ri\right) \tag{1}$$

$$\frac{\Delta i}{\Delta v}(s) = \frac{1}{R + Ls} \tag{2}$$

The electromechanical response of the SPC is defined by the swing equation of a rotating mass with damping, as in (3), where ω is the rotor speed, J is its moment of inertia, D is the damping coefficient of the machine and P_{mech} and P_{elec} are respectively the input and output power. However, in the case of a converter, it is possible to modify the moment of inertia and the damping coefficient in real time in order to adapt them to power system conditions.

$$J\frac{d\omega}{dt} = \frac{P_{mech} - P_{elec}}{\omega} - D\Delta\omega \tag{3}$$

Therefore, the SPC employs a small signal version of (3), given by (4). In this equation, ω is approximated by the rated angular speed ω_g and T_P is the coefficient linking small angle and active power variations. This results in the active power loop shown in Fig. 4, and the corresponding closed-loop transfer function is (5), with the desired moment of inertia and damping coefficient.

$$\frac{\Delta\omega}{\Delta P}(s) = \frac{1}{J\omega_g}\frac{1}{s + 2\zeta\sqrt{\frac{T_P}{J\omega_g}}} \tag{4}$$

$$\frac{\Delta P_{out}}{\Delta P_{ref}}(s) = \frac{\frac{T_P}{J\omega_g}}{s^2 + 2\zeta\sqrt{\frac{T_P}{J\omega_g}}s + \frac{T_P}{J\omega_g}} \tag{5}$$

Both the electrical and the electromechanical characteristic of the SPC have an increased flexibility with respect to their corresponding systems in conventional synchronous generators. The SPC allows setting the values of resistance, inductance, moment of inertia and damping coefficient, and even modifying them in real time.

Finally, the reactive power controller is materialized as a proportional, integral controller that cancels the error in the reactive power injection by modifying the value of the internal voltage magnitude E.

3) Higher-level controllers: Additionally, the active and reactive power references required by the SPC can be modified by higher-level controllers in order to perform frequency and voltage regulation. In this case, a frequency droop modifying the active power reference and a local bus voltage droop modifying the reactive power reference are considered, as indicated in (6) and (7).

$$\Delta P_{droop} = K_f\left(f_{ref} - f\right) \tag{6}$$

$$\Delta Q_{droop} = K_v\left(V_{ref} - V\right) \tag{7}$$

TABLE II
PER UNIT CHARACTERISTICS OF CABLES

Cable	R (pu)	X (pu)
0-1, 0-6	$8.430 \cdot 10^{-4}$	$1.381 \cdot 10^{-3}$
1-2, 6-7	$3.512 \cdot 10^{-4}$	$5.753 \cdot 10^{-4}$
2-3, 7-8	$5.725 \cdot 10^{-4}$	$6.217 \cdot 10^{-4}$
3-4, 8-9	$5.725 \cdot 10^{-4}$	$6.217 \cdot 10^{-4}$
4-5, 9-10	$8.857 \cdot 10^{-4}$	$6.648 \cdot 10^{-4}$

III. Power Plant Equivalent Model

A. Electrical equivalent

The equivalent model of the power plant is developed in per unit for a 33 kV base voltage and a 20 MVA base power. Therefore, the starting point is the per unit single-line diagram of the plant shown in Fig. 5. In this diagram, C_{i-j}, $T_{i\alpha}$ and $\underline{Z}_{i\alpha}$ respectively represent sections of cable, transformers and SPC virtual impedances, $\underline{E}_{i\alpha}$ are the SPC internal voltages and $\underline{V}_{i\alpha}$ indicate converter terminal voltages. The per unit values of the impedances associated to C_{i-j} are given in Table II and the transformer per unit impedance is $\underline{Z}_{tr} = 0.05217 + 1.565j$, whereas the virtual impedance and the internal voltage of the converters have to be considered as variables.

The objective of the equivalent model is to represent the plant as an SPC converter with its internal voltage and virtual impedance, behind the equivalent impedance of cables and transformers.

First, looking at Table II and comparing the cable impedance with the transformer impedance, it is possible to neglect the impedance of the cables in the aggregated model because it represents a small fraction of the impedance of the transformers. Therefore, it is interesting to consider the general model in Fig. 6 and its Thévenin equivalent given by (8).

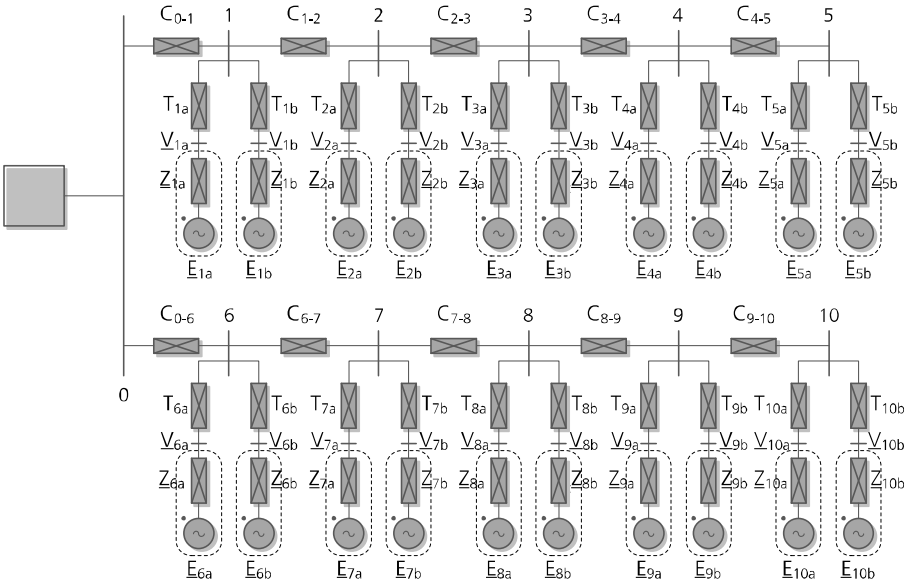

Fig. 5. Per unit single-line diagram of the power plant.

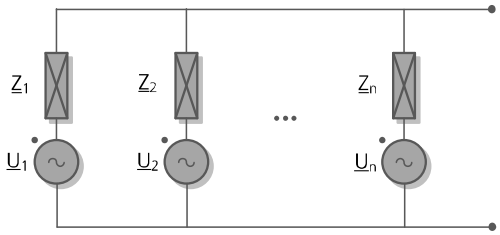

Fig. 6. Single-line diagram of a system formed by an arbitrary number of voltage sources connected to a common bus.

$$\underline{U}_{th} = \frac{\sum_{k=1}^{n} \frac{\underline{U}_k}{\underline{Z}_k}}{\sum_{k=1}^{n} \frac{1}{\underline{Z}_k}} \qquad \underline{Z}_{th} = \frac{1}{\sum_{k=1}^{n} \frac{1}{\underline{Z}_k}} \tag{8}$$

Applying (8) with $\underline{U}_k = \underline{V}_{i\alpha}$ and $\underline{Z}_k = \underline{Z}_{tr}$ for all k, it is possible to obtain the equivalent impedance representing the transformers, which is given by (9). With this, the plant can be represented by a new simplified model consisting of the equivalent transformer impedance $\underline{Z}_t$, a common bus and the SPC converters with their virtual impedance and internal voltage. Therefore, it is possible to utilize the model in Fig. 6 again to determine the equivalent virtual impedance $\underline{Z}_v$, which is a function of all the SPC virtual impedance values given by (10).

$$\underline{Z}_t = \frac{\underline{Z}_{tr}}{20} = 0.002609 + 0.07826j \tag{9}$$

$$\underline{Z}_v = \frac{1}{\sum_{i=1}^{10} \left(\frac{1}{\underline{Z}_{ia}} + \frac{1}{\underline{Z}_{ib}} \right)} \tag{10}$$

B. Electromechanical equivalent

The equivalent model of the virtual internal voltage source requires calculating the corresponding electromechanical parameters and reactive power controller gains.

The equivalent machine must represent the total inertia of the plant. Therefore, its per unit inertia H is given by (11), where $H_{i\alpha}$ and $S_{b,i\alpha}$ are respectively the per unit inertia (in seconds) and the base power for each converter and $S_{b.plant} = 20\,\text{MVA}$ is the base power of the plant. In this case, all converters share a common base power $S_{b,i\alpha} = 1\,\text{MVA}$, so H is exactly the average of all $H_{i\alpha}$.

$$H = \frac{\sum_{i=1}^{10} (H_{ia} S_{b,ia} + H_{ib} S_{b,ib})}{S_{b,plant}} \tag{11}$$

With this inertia, and taking into account the left-hand side of (3), it is also possible to define an equivalent frequency for the plant. It corresponds to the center of inertia of the plant and is given by (12). Additionally, the equivalent damping of the power plant can be calculated to maintain the steady-state relation between active power and frequency resulting from (4).

$$f = \frac{\sum_{i=1}^{10} (f_{ia} H_{ia} S_{b,ia} + f_{ib} H_{ib} S_{b,ib})}{H S_{b,plant}} \tag{12}$$

TABLE III
STATION PARAMETERS AND ACTIVE POWER REFERENCES

Station	R (pu)	X (pu)	H (pu)	P_{ref} (pu)
$1a$	0.025	0.15	2.5	0.80
$1b$	0.025	0.15	2.5	0.83
$2a$	0.025	0.15	2.5	0.60
$2b$	0.025	0.15	2.5	0.77
$3a$	0.025	0.15	2.5	0.73
$3b$	0.025	0.15	2.5	0.63
$4a$	0.050	0.30	2.5	0.44
$4b$	0.050	0.30	2.5	0.56
$5a$	0.050	0.30	2.5	0.52
$5b$	0.050	0.30	2.5	0.42
$6a$	0.100	0.60	5.0	0.83
$6b$	0.100	0.60	5.0	0.80
$7a$	0.100	0.60	5.0	0.77
$7b$	0.100	0.60	5.0	0.60
$8a$	0.050	0.30	5.0	0.63
$8b$	0.050	0.30	5.0	0.73
$9a$	0.050	0.30	5.0	0.56
$9b$	0.050	0.30	5.0	0.44
$10a$	0.050	0.30	5.0	0.42
$10b$	0.050	0.30	5.0	0.52
Equivalent	0.0417	0.25	3.75	0.63

The reactive power controller gains, on the other hand, are calculated proportionally to the value of the reactance seen by each SPC converter, so the same proportionality ratio is kept for the equivalent model, using the reactance values in $\underline{Z}_t$ and $\underline{Z}_v$.

Finally, the droop slope K_f and K_v of the equivalent machine must be such that they reproduce the aggregated response of the plant. Since they are also defined in terms of per unit power, their calculation is analogous to the case of the moment of inertia and they are obtained as the average value of the droop slopes of all converters.

IV. RESULTS

The performance of the equivalent model has been validated against the detailed model of the plant. The study has been carried out with DIgSILENT PowerFactory and in this simulation the SPC parameters and active power references are different among the stations, as given by Table III, where station parameters are expressed in per unit using the station base, that is to say, a base power of 1 MVA, whereas the parameters of the equivalent model are expressed in the plant base of 20 MVA. The damping ratio of each machine is 0.8, but due to their different inertia and impedance values, the damping ratio of the aggregate response is 0.85. Finally, both the frequency and voltage droop coefficients are 5% and the reactive power reference is 0 for all the stations and the equivalent converter.

A. Response to a step

The first test compares the power injections of both models when the active and reactive power references are modified with step variations. The total plant active power reference is increased by 15% at $t = 1$ s, and afterwards the reactive power reference increases from 0 to 0.45 pu at $t = 3$ s.

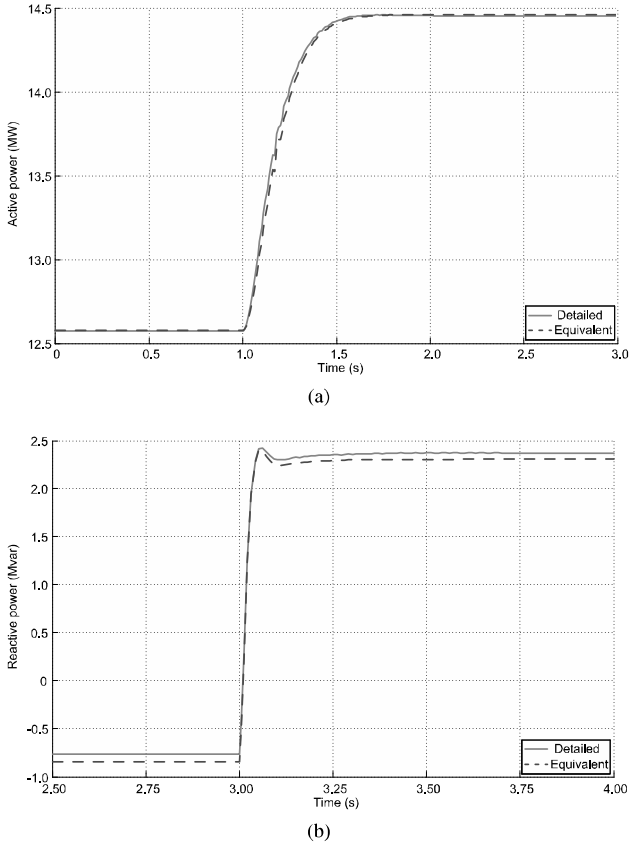

Fig. 7. Power injections of the detailed model (solid line) and the equivalent model (dashed line) of the plant: (a) Active power response to a step at $t = 1$ s. (b) Reactive power response to a step at $t = 3$ s.

Fig. 7 shows the active and reactive power injections of the detailed and equivalent models of the plant that result from these disturbances. It is possible to see how the response of the equivalent model tracks the response of the detailed model with accuracy.

In Fig. 7a, the active power injected by the plant equivalent model reproduces the dynamics of the P injection in the detailed model with slight differences during the transient. In fact, these differences are below 0.14 MW, which corresponds to 0.7% of the rated power of the plant.

On the other hand, Fig. 7b shows the reactive power response of both models, which does not reach its reference because of the droop response of the plant and the voltage rise due to P and Q injections. In this case it is possible to see a small steady-state difference between both models. The maximum error is 0.10 Mvar, i.e., 0.5% of the rated power of the plant.

Therefore, the errors introduced by the equivalent model, below 1% of the rated power of the plant, can be considered acceptable.

Additionally, it is interesting to analyze the relation between

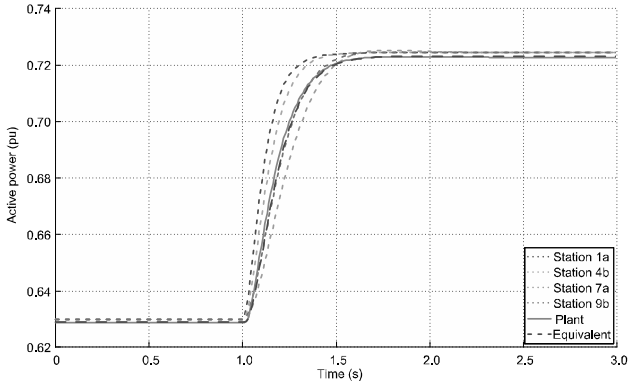

Fig. 8. Power response of representative stations compared to the plant power response in the detailed and the equivalent model.

the individual power responses of the stations and the total plant power response, considering also the equivalent model. In order to compare all power responses in a common frame, Fig. 8 plots the active power responses of four representative stations and the plant when all the stations are initially injecting $0.63\,\mathrm{pu}$ active power and the total plant reference is increased again by 15% at $t = 1\,\mathrm{s}$. Fig. 8 shows how stations with higher values of inertia and impedance react more slowly, since they oppose more strongly to changes. The total plant response and the response of the equivalent model are an average value of these responses, slightly displaced downwards due to the losses in the transformers and cables.

B. Response to a frequency ramp

In the second test, the accuracy of the equivalent model is studied under a ramp variation in the grid frequency. At $t = 1\,\mathrm{s}$, the grid frequency starts to increase at a constant pace until it reaches a value of $1.002\,\mathrm{pu}$ at $t = 3\,\mathrm{s}$; afterwards, this value is kept constant for the rest of the test.

Fig. 9 shows the effect of the grid frequency disturbance on the internal frequency of the converters in the plant and the total active power injection. In the case of the detailed model, the frequency is calculated taking into account (12), whereas the active power is measured at the actual point of connection of the plant.

In Fig. 9a, the frequency of the plant follows the grid frequency with certain delay, which is due to the effect of the emulated inertia. The results are very similar for both models, with a maximum difference between them of $10^{-5}\,\mathrm{pu}$. Therefore, the equivalent converter represents the center of inertia of the plant with great accuracy.

The resulting active power injection is plotted in Fig. 9b. The active power generated by the plant decreases as the measured frequency increases, from $12.6\,\mathrm{MW}$ down to a value around $6.5\,\mathrm{MW}$. This reduction is due to the external droop loop and the effect of the steady-state gain of the transfer function introduced in (4), which further contributes to frequency regulation with an additional decrease of the active power output when the frequency is too high. The comparison

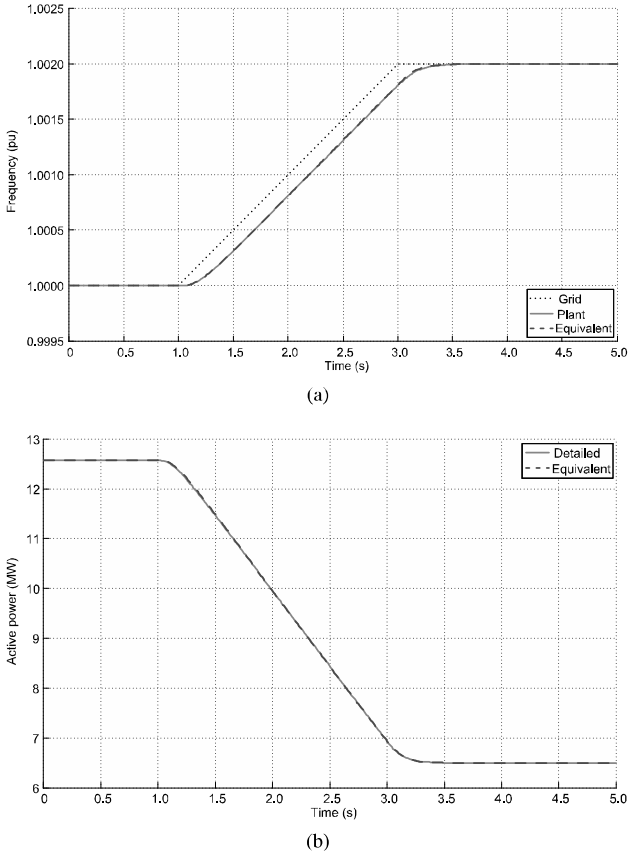

Fig. 9. Response of the detailed model (solid line) and the equivalent model (dashed line) of the plant to a grid frequency ramp: (a) Internal frequency. (b) Active power injection.

between both models is again satisfactory, with a maximum error below $0.03\,\mathrm{MW}$, which is 0.015% of the rated power of the plant.

Since the dynamics of the internal frequency and the active power injection are linked, it is possible to analyze the evolution of both variables at the same time during this frequency ramp. At the beginning of the ramp, the internal frequency is close to its original value and the grid frequency increases. This decreases the angle by which the plant leads the grid, which in turn reduces the output active power. Meanwhile, the active power reference remains almost unaffected, so the virtual rotor starts to accelerate because of the output power reduction, although the acceleration rate is constrained by the moment of inertia. During the ramp, the internal frequency continues increasing, which reduces the active power reference because of the droop. In fact, the active power balance stabilizes around a constant difference between the input and output power that results in a constant acceleration of the virtual rotor. When the grid frequency becomes constant again, the internal frequency continues increasing until it reaches the same value. However, the acceleration during the last part of the transient is less accused because the active power imbalance is progressively canceled.

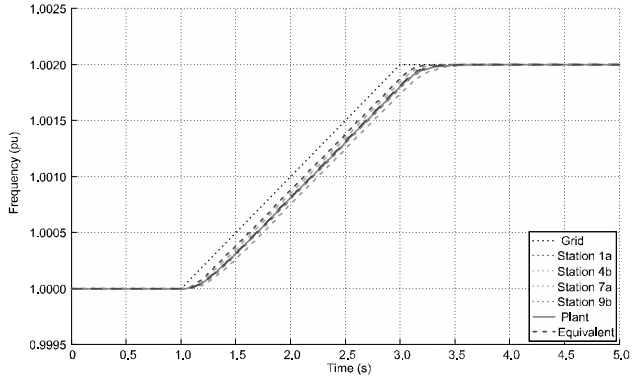

(a)

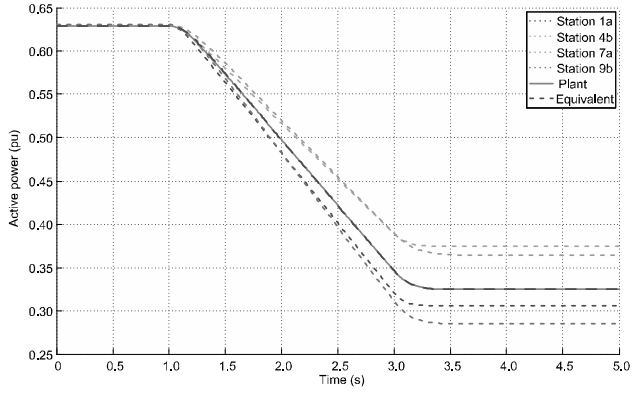

(b)

Fig. 10. Response of representative stations compared to the plant response in the detailed and the equivalent model: (a) Internal frequency. (b) Active power injection.

As in the previous case, in order to compare the response of individual generating units with the total response of the plant obtained by both models, a simulation of the same event when all the stations are initially injecting 0.63 pu active power has also been carried out. The results are shown in Fig. 10.

On the one hand, Fig. 10a shows how the internal frequency of four stations with different parameters behaves, compared to the plant frequency. Stations with less inertia and impedance are faster and track the grid frequency more closely. The plant frequency obtained with both models has an intermediate performance, with the same evolution as in the test with different power references for each station.

On the other hand, the active power response is shown in Fig. 10b. Initially, all the machines, and also the plant, inject 0.63 pu. However, as the grid frequency starts to increase, the stations react differently due to their different inertia. When the ramp finishes and the system reaches a new steady state, the machines inject different amounts of active power. This is due to the steady-state gain of the transfer function in (4), which is modified by the inertia and the impedance of each machine. The right adjustment of the damping ratio allows the equivalent model to reproduce the active power injection of the power plant.

V. Conclusion

This paper presents a PV power plant constituted by 20 power conversion stations of 1 MW that employ the synchronous power controller. The synchronous power controller allows converters to interact synchronously with the power system, being able to provide the same services as conventional generators while avoiding some of their drawbacks, like their slightly damped nature. Taking into account the topology of the plant and the structure of the controller, an equivalent model of the plant is derived. This equivalent model aggregates all the converters in the plant as a single one controlled by the synchronous power controller by analyzing the Thévenin equivalent of the plant and its total inertia and regulation contribution.

The equivalent model has been compared with the detailed one through simulation of different disturbances like step changes of the active and reactive power of the plant or a grid frequency ramp. The obtained results show that it is able to reproduce the response obtained with the complete model with great accuracy. In fact, the maximum error in the active and reactive power injection is below 1% of the rated power of the plant, whereas the frequency estimation error is around 10^{-5}. Therefore, this equivalent model is highly valuable, as it provides the necessary tool to analyze the impact of the plant on large power systems.

References

[1] International Energy Agency, *World Energy Outlook 2014*. Paris: OECD/IEA, 2014.

[2] P. Kundur, *Power System Stability and Control*. New York: McGraw-Hill, 1994.

[3] *ENTSO-E Network Code for Requirements for Grid Connection Applicable to all Generators*, ENTSO-E Std., Mar 2013.

[4] H. Bevrani, T. Ise, and Y. Miura, "Virtual synchronous generators: A survey and new perspectives," *Electrical Power and Energy Systems*, vol. 54, pp. 244–254, 2014.

[5] L. Zhang, L. Harnefors, and H.-P. Nee, "Power-synchronization control of grid-connected voltage-source converters," *Power Systems, IEEE Transactions on*, vol. 25, no. 2, pp. 809–820, May 2010.

[6] C.-H. Zhang, Q.-C. Zhong, J.-S. Meng, X. Chen, Q. Huang, S.-H. Chen, and Z. peng Lv, "An improved synchronverter model and its dynamic behaviour comparison with synchronous generator," in *Renewable Power Generation Conference (RPG 2013), 2nd IET*, Sept 2013, pp. 1–4.

[7] P. Rodriguez, I. Candela, and A. Luna, "Control of PV generation systems using the synchronous power controller," in *Energy Conversion Congress and Exposition (ECCE), 2013 IEEE*, Sept 2013, pp. 993–998.